Helvetica Chimica Acta

HELVETICA chimica acta

PERSPECTIVE OPEN ACCESS

Mixed Ionic–Electronic Conduction in Layered Hybrid Halide Perovskites

Ghewa AlSabeh[1] | Algirdas Dučinskas[1] | Jovana V. Milić[2] | Michael Graetzel[1]

[1]Laboratory of Photonics and Interfaces, Ecole Polytechnique Fédérale de Lausanne, Lausanne, Switzerland | [2]Department of Chemistry, University of Turku, Turku, Finland

Correspondence: Jovana V. Milić (jovana.milic@utu.fi) | Michael Graetzel (michael.graetzel@epfl.ch)

Received: 8 December 2025 | **Revised:** 11 May 2026 | **Accepted:** 22 May 2026

Keywords: layered halide perovskites | material design | mixed ionic–electronic conductors | operational stability | phase segregation

ABSTRACT

Mixed ionic–electronic conductivity of metal halide perovskites is a critical factor determining their application in optoelectronics, as well as the emerging field of optoionics. In particular, ionic migration in response to voltage bias and light contributes to the operational instability of halide perovskite materials and devices. A promising strategy to control ion migration is dimensional reduction, achieved by incorporating bulky organic cations between inorganic slabs to form two-dimensional or layered hybrid halide perovskites. In this perspective article, we discuss the mixed conductivity of layered halide perovskite materials and the impact on the operational stability of perovskite optoelectronics and emerging applications.

1 | Introduction

Hybrid metal halide perovskites have emerged as prominent semiconductors featuring excellent optoelectronic properties [1–4], mechanical flexibility, and low-cost fabrication [5, 6], promising for next-generation photovoltaics [5, 7–9]. They are based on the general formula AMX_3 defining a corner-shared $\{MX_6\}$ octahedral framework (Figure 1a) with central monovalent cations A that are either organic (e.g. methylammonium (MA^+), formamidinium (FA^+)), or inorganic (e.g. Cs^+), divalent metal cations M (Pb^{2+}, Sn^{2+}), and halide anions X^- (I^-, Br^-, Cl^-) [2, 10]. These mixed ionic–electronic conductors exhibit exceptional optoelectronic properties [2, 11], including strong light absorption, long charge carrier lifetimes, high diffusion lengths, and large defect tolerance even when produced by simple solution processing [1, 2, 12]. Despite their extraordinary performance in photovoltaics, metal halide perovskites suffer from poor long-term stability [6, 13], which limits their application. Their performance can decline when exposed to moisture, oxygen, heat, or light, leading to their degradation [6, 14]. This is often due to ion migration within the perovskite lattice, which has been identified as a major cause of instability [15, 16]. Specifically, mobile ions such as halides and A-site cations can migrate under the electric field or illumination [17], causing current–voltage hysteresis, interfacial reactions, and phase segregation, which can induce degradation and impair stability [18–20]. The overall effect can be detrimental, making control of ionic migration crucial for perovskite solar cells [17, 21]. A variety of strategies have been developed to mitigate ion migration in metal halide perovskites (Figure 1b–d) [22, 23]. One of the most effective approaches has been the incorporation of bulky organic cations that can modulate the perovskite interface (Figure 1b) or template low-dimensional (2D) or layered hybrid halide perovskite (LHP) architectures (Figure 1c–d) [24–27], which exhibit improved operational

The opinions expressed in this publication are the view of the author(s) and do not necessarily reflect the opinions or views of Helvetica Chimica Acta, the Publisher, the Society, or the affiliated editors.

Dedicated to the Swiss Chemical Society on the occasion of their 125th birthday.

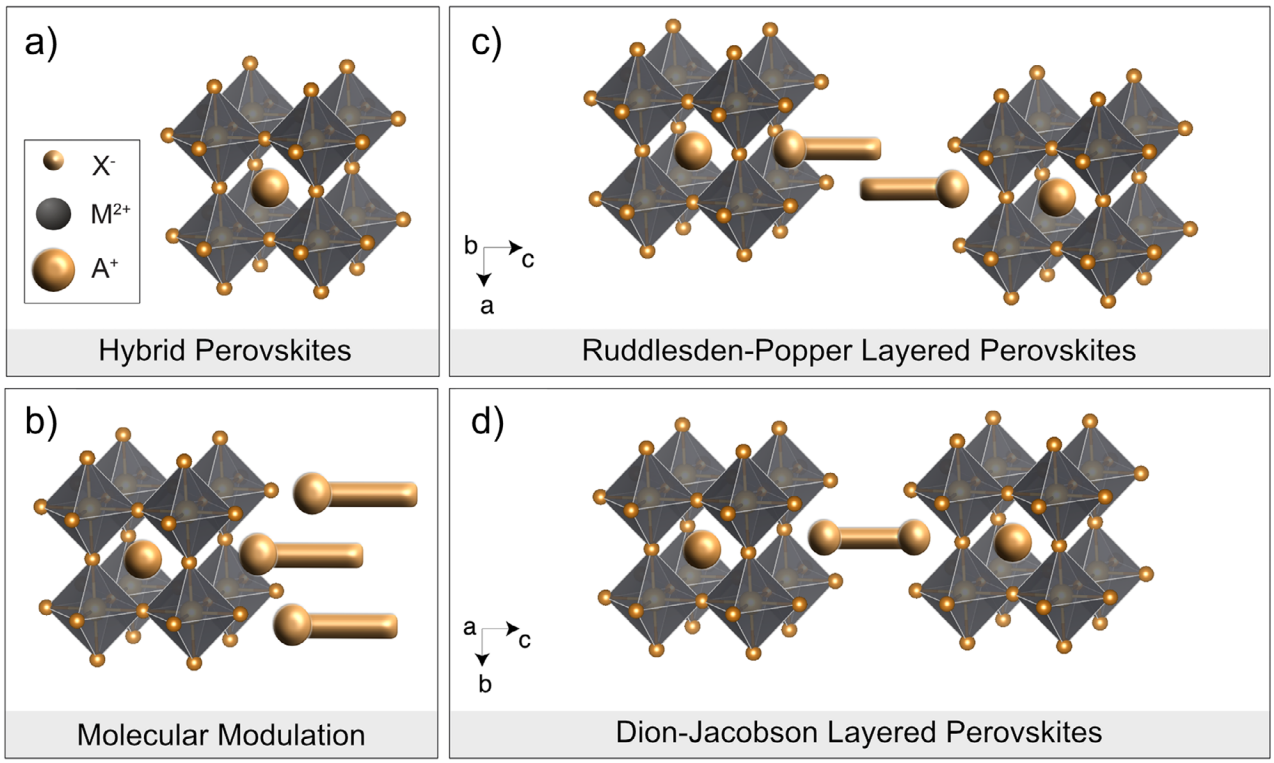

FIGURE 1 | Schematic representation of the structure of (a) hybrid halide perovskites and their (b) molecular modulation, as well as (c–d) layered perovskite analogues, including the (c) RP and (d) DJ phases (adopted from the Ref. [33]). Copyright 2022 Royal Society of Chemistry.

stability [28, 29]. In these structures, inorganic perovskite slabs are separated by organic spacer layers, forming low-dimensional haloplumbate phases [29]. Among these, the Ruddlesden–Popper (RP; Figure 1c) [30] and Dion–Jacobson (DJ; Figure 1d) [31] phases have received the most attention [32]. Their general formula is $S_xA_{n-1}M_nX_{3n+1}$, where organic spacer cation (S) can be monofunctional ($x = 2$) or bifunctional ($x = 1$) alkylammonium cations [32]. Structurally, RP phases feature a half-unit–cell shift between adjacent perovskite layers, whereas DJ phases are aligned without such displacement [32]. Despite the increased hydrophobicity and ion-impermeability of the organic layer, LHPs remain mixed ionic–electronic conductors, with ionic transport influencing their optoelectronic properties and stability [30, 32].

Here, we review the mixed conductivity of LHP materials and discuss the methods for assessing it. Moreover, we address the impact of mixed conduction on optoelectronic properties, device performance, and operational stability, as well as emerging applications.

2 | LHPs as Mixed Conductors

In contrast to conventional semiconductors, LHPs exhibit mixed ionic and electronic conductivity [24]. The inorganic slabs provide pathways for electronic transport, often with strong in-plane anisotropy, while point defects, such as halide vacancies and interstitials (Figure 2), enable ionic migration within the lattice and between layers. Although LHPs tend to suppress ion migration relative to their 3D counterparts, the ionic mobility significantly influences their optoelectronic characteristics and device performance [28]. Understanding the interplay of ionic and electronic processes is therefore essential for optimizing these materials in photovoltaics, light-emitting devices, and emerging ionic–electronic hybrid technologies [14, 34]. Extensive investigations into the electrical properties of 3D $MAPbI_3$ have consistently pointed to iodide vacancies as the dominant mobile ionic species, owing to their low formation energy and migration barrier [35]. However, the precise nature of the prevailing defect disorder remains under debate [36], as both anti-Frenkel [37] and intrinsic Schottky-type [38] defects have been proposed as plausible mechanisms. In the anti-Frenkel scenario, a halide ion migrates from its lattice site to an interstitial position, forming a vacancy-interstitial pair that contributes to ionic transport. In contrast, an intrinsic Schottky-type defect involves the formation of charge-compensated cation and anion vacancies. Among these, intrinsic Schottky disorder is more widely accepted, supported by experimental evidence indicating a substantial concentration of MA vacancies, which are believed to compensate for halide vacancies in $MAPbI_3$ [39]. Building on this understanding, the extent to which these defect mechanisms persist or are modified in LHPs remains an important question. While this defect chemistry is often assumed to be comparable in LHPs [24, 26], the manifestation of these defects is strongly influenced by reduced dimensionality and structural confinement imposed by organic spacer layers [32]. In this context, ionic transport in halide perovskites can, in principle, proceed via both interstitial (anti-Frenkel) and vacancy-mediated (Schottky) mechanisms. However, consistent with observations in 3D systems, vacancy-mediated migration, particularly of halide ions, is generally considered the dominant transport pathway [40]. In LHPs, ionic transport is further modified by structural confinement imposed by bulky organic spacer layers, which hinder ion migration

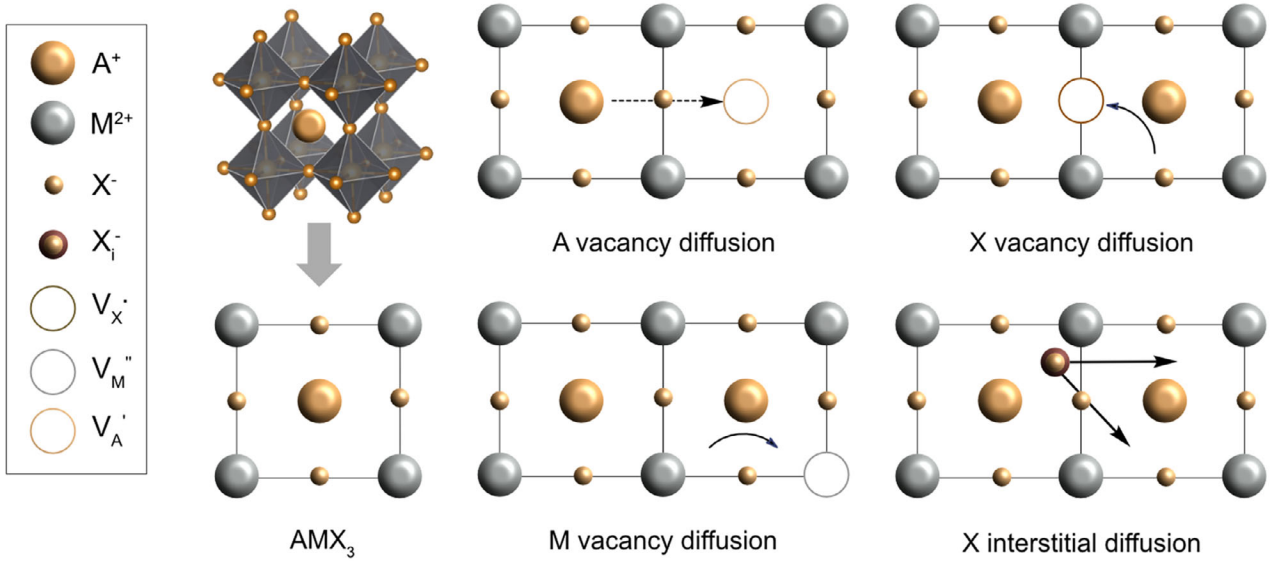

FIGURE 2 | Schematic illustration of ion migration in metal halide perovskites mediated by defect diffusion. Spheres represent lattice ions occupying A, M, and X sites, while open circles denote vacancies ($V_X^{\cdot}$, $V_M^{''}$, $V_A^{'}$) and shaded spheres with a halo indicate interstitial species (X_i). Migration pathways for A-site, M-site, and halide (X) ions are shown for both vacancy- and interstitial-mediated diffusion mechanisms.

compared to their 3D counterparts [41]. As a result, ionic conduction in LHPs is expected to be primarily governed by vacancy diffusion, while interstitial-mediated transport is likely energetically less favorable due to steric and electrostatic constraints within the layered structure. Consequently, ion migration is also anisotropic, occurring mainly within the inorganic layers while mostly hindered across the organic spacers, which can lead to ion accumulation at interfaces and affect device stability [42]. For instance, LHPs incorporating *n*-butylammonium (BA) spacer cations demonstrate significantly reduced ion migration along the in-plane direction compared to their 3D counterparts, primarily due to the organic spacer layers constraining ionic movement [43].

Temperature-dependent conductivity measurements reveal that 3D $MAPbI_3$ single crystals show a clear transition from electronic to ionic conduction at temperatures above 280 K, with an activation energy for ionic conduction of 0.83 eV in the dark and 0.33 eV under illumination. In contrast, quasi-2D $BA_2MA_2Pb_3I_{10}$ perovskites maintain a constant activation energy of 25 ± 3 meV across the entire temperature range (up to 350 K), with no transition to ionic conduction. This absence of ionic conduction quantitatively demonstrates suppressed ion migration in the layered structure. This suppression is attributed to a lower concentration of point defects, specifically methylammonium (V_{MA}) and iodide (V_I) vacancies within the RP-type perovskite. Density functional theory (DFT) calculations reveal that the formation energies of these vacancies are significantly higher in quasi-2D $BA_2MA_2Pb_3I_{10}$ than in 3D $MAPbI_3$: 5.72 eV vs. 6.94 eV for V_{MA} and 3.44 eV vs. 5.46 eV for V_I, respectively [43]. The higher formation energies associated with these vacancies relative to those in $MAPbI_3$ hinder defect generation and, consequently, limit ionic transport within the lattice. In another study with 2D $(BA)_2(MA)_3Pb_4I_{13}$ films, no transition from electronic to ionic conductivity was observed when the temperature increased up to 330 K, both under dark and illuminated conditions [23]. The activation energy for conductivity in these films remained at 41 ± 7 meV, indicating purely electronic transport without any transition to ionic conductivity. This behavior contrasts with 3D $CH_3NH_3PbI_3$, where ionic conduction emerges at temperatures above 260 K (dark) and 240 K (illuminated), with activation energies of 0.19 eV (dark) and 0.03 eV (illuminated). The increased formation energies of point defects lead to fewer mobile ions, thereby further suppressing ionic migration within the perovskite layers. The conductivity behavior within this range indicates purely electronic transport, confirming the effective suppression of ion migration in these LHP films. This reduction in ionic mobility is attributed to organic spacer layers that act as barriers to ion movement, although contributions from the unique grain boundary geometry in 2D structures cannot be ruled out [23]. Likewise, halide migration in systems employing 2-phenylethylammonium (PEA) spacers becomes easier as the layer number (n) increases. Lower-n 2D structures exhibit higher activation energies ranging from 72 kJ/mol (n = 1) to 58 kJ/mol (n = 10) due to the confinement and blocking effect of organic spacer layers, effectively suppressing ion migration and enhancing material stability [44]. The absence of significant ion migration mitigates several detrimental effects commonly observed in 3D perovskite devices, including photocurrent hysteresis, photoinduced poling, light-induced phase separation, and ion-driven degradation of charge transport layers and electrodes [45]. Moreover, the hydrophobic nature of the BA and PEA cation chains, as well as other spacers, likely enhances resistance to moisture and oxygen ingress, further improving overall durability. Overall, these findings highlight that reduced dimensionality effectively suppresses ionic transport in LHPs while preserving mixed conduction, emphasizing the critical role of structural confinement in controlling ion migration. This balance between suppressed ionic mobility and maintained electronic conductivity is key to attaining stable and high-performing optoelectronic devices.

Unlike RP LHPs, DJ systems incorporate bifunctional spacers and are gaining attention for their enhanced thermal stability

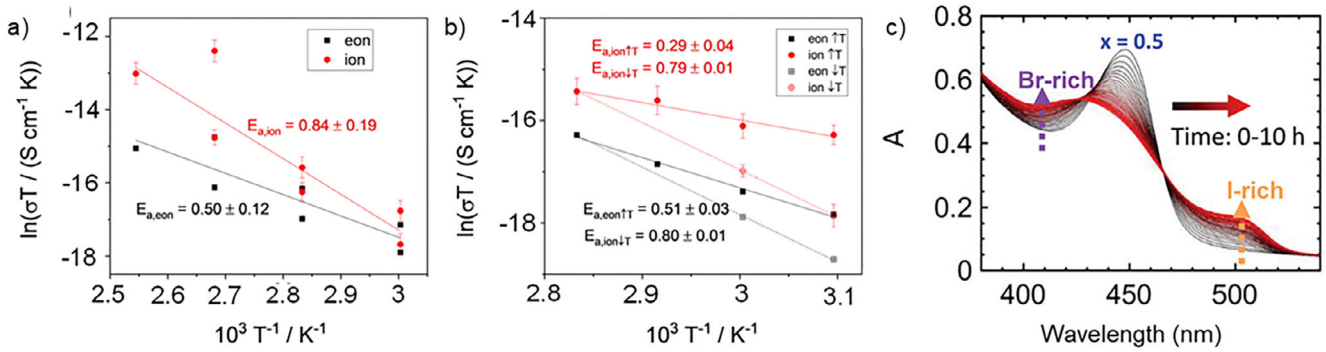

FIGURE 3 | Mixed-conduction measurements of LHPs. Arrhenius plots of (a) $(PDMA)PbI_4$ and (b) $(BzA)_2PbI_4$ perovskites for electronic (*eon*, black) and ionic (*ion*, red) charge carrier transport obtained from conductivity measurements (adopted from the reference [24]). Copyright 2024 Royal Society of Chemistry. (c) Halide phase segregation upon illumination is shown through the UV–vis spectra evolution of $(PDMA)Pb(I_{0.5}Br_{0.5})_4$ thin films under light (1.5 mW cm^{-2}) at 80°C for ≈10 h with 20 min intervals (adopted from the Ref. [47]). Copyright 2022 John Wiley and Sons.

with potential in optoelectronics [24, 31, 46]. This enhanced stability of DJ perovskites has been attributed to the absence of van der Waals spacer bilayers, shorter interlayer distances, and stronger hydrogen bonding between the organic spacer and inorganic layers, which together improve structural rigidity and resistance to degradation, as supported by experimental studies reporting improved stability under humidity, thermal stress, and illumination [24, 42, 46]. Nevertheless, RP perovskites can also exhibit comparable stability under certain conditions, depending on factors such as spacer chemistry, layer thickness, and environmental conditions [42]. Dučinskas et al. compared the mixed ionic–electronic transport properties of RP-type benzylammonium (BzA) based $(BzA)_2PbI_4$ and DJ-type 1,4-phenylmethylammonium (PDMA) containing $(PDMA)PbI_4$ thin films comprising aromatic organic spacers (Figure 3a). Using in-plane measurements combining direct current (DC) polarization and impedance spectroscopy under controlled iodine partial pressures, ionic and electronic contributions to conduction were evaluated along with their activation energies (Figure 3b). Both materials exhibited mixed conduction, but with significantly lower ionic and electronic conductivities than those of the corresponding 3D perovskites, confirming that reduced dimensionality suppresses charge transport. The DJ perovskite showed higher activation energies for both transport types (≈ 0.4–0.5 eV for electronic and ≈ 0.8 eV for ionic conduction) and superior thermal stability, remaining structurally intact up to ~150°C. Similarly, AlSabeh et al. showed that aryl-acetylene-based LHPs display mixed ionic–electronic conduction, yet with electronic conductivities below the measurable detection limit [25]. They further demonstrated that the ionic conductivity is substantially lower than in 3D $MAPbI_3$, which is attributed to the larger interlayer spacing characteristic of 2D perovskites. Building on these insights into the ionic and electronic transport characteristics of LHPs with aromatic organic spacers, Wang et al. further examined how light influences the halide distribution and phase stability in DJ mixed halide perovskites [47]. They revealed that, despite the reduced ionic mobility inherent to the layered architecture, illumination can still drive reversible halide segregation in $(PDMA)Pb(I_{0.5}Br_{0.5})_4$ films, leading to the formation of distinct iodide- and bromide-rich domains. This photo-de-mixing process changes the optical absorption (Figure 3c) and remains kinetically trapped in the dark at room temperature yet fully returns to the mixed state upon mild heating, demonstrating thermodynamic reversibility. Temperature-dependent analyses identified a photo-miscibility gap that widens at lower temperatures, underscoring the persistent coupling between light exposure, ion mobility, and phase thermodynamics. These findings show that, while dimensional reduction in DJ perovskites effectively suppresses ion transport under equilibrium conditions, light can still activate optoionic effects, posing a challenge to long-term stability and offering an opportunity for new functionalities. From a thermodynamic perspective, halide segregation in mixed-halide perovskites arises from the competition between the enthalpic penalty of mixing (associated with lattice mismatch between I^- and Br^-) and the entropic stabilization of the homogeneous phase [48, 49]. Under illumination, this balance is altered by an additional electronic free-energy contribution, as photocarriers preferentially localize in lower-bandgap iodide-rich regions, thereby stabilizing phase-separated domains and giving rise to a photo-miscibility gap [48]. In 3D mixed-halide perovskites, this process is facilitated by high ionic mobility, leading to rapid and reversible segregation [50]. In contrast, reduced dimensionality in layered (2D) systems suppresses ion transport and slows the kinetics of both segregation and recovery, yet does not eliminate the thermodynamic driving force under illumination [51]. As a result, photo-induced de-mixing can still occur in DJ perovskites, but with enhanced kinetic stability of the demixed state and stronger temperature dependence of the miscibility gap [51]. Together, these results demonstrate that both structural design and external stimuli, such as light, play a critical role in tuning ionic transport and phase stability in LHPs. This demonstrates the need to carefully consider optoionic effects when designing layered perovskites for stable and efficient device operation.

Dimensionality reduction in LHPs offers an effective approach to reducing ion migration, and RP and DJ phases exhibit conductivities several orders of magnitude lower (≈10^{-6}–10^{-9} S cm^{-1}) than 3D $MAPbI_3$ [52, 53]. This reduction in conductivity arises primarily from their wider band gaps, which limit the concentration of thermally activated charge carriers, and from carrier confinement effects intrinsic to the layered structures. Such effects are less pronounced in quasi-2D perovskites (n > 1), where the structure approaches that of 3D perovskites. The lower ionic conductivity of LHPs can similarly be linked to factors such as higher defect formation energies, anisotropic ion

migration pathways, and increased ion migration barriers [54]. The activation energy (E_a) governing these processes therefore reflects a combination of migration and formation contributions, the relative significance of which depends on the defect type (Figure 2) and local structure [55]. For electronic carriers, with often negligible migration barriers, E_a effectively corresponds to the thermal excitation (formation) energy. In hybrid halide perovskites, however, ionic motion remains substantial, suggesting that the activation energies of ionic defects are not sufficiently high to suppress ion migration completely. Reported E_a values for iodide transport in $MAPbI_3$ typically fall within the range of 0.2–0.6 eV, although these vary widely depending on composition, microstructure, and measurement conditions [39, 52, 56]. For instance, partial substitution of the A-site cation can either increase or decrease E_a, while grain boundaries often facilitate ion migration and thus reduce the overall barrier [22, 57]. Importantly, dimensionality reduction has been identified as an effective route to enhance the E_a and stabilize the lattice against ion migration [24]. This is evident in DJ-type perovskites, which have superior thermal stability compared with their RP counterparts, owing to key structural differences. In RP phases, the presence of a van der Waals gap between organic layers and weakly bound spacer molecules makes the lattice more vulnerable to thermal stress and degradation. In contrast, DJ perovskites incorporate bifunctional spacers that eliminate the van der Waals gap, producing shorter interlayer distances and a more rigid framework. These stronger interlayer interactions and reduced structural flexibility not only enhance stability at elevated temperatures but also correlate with the higher E_a often observed for ion migration, making DJ perovskites more robust and promising for protective layers [24, 58, 59]. The comparison between the different phases requires systematic investigation via complementary methods.

It is important to note that the wide variation in reported activation energies for ion migration in metal halide perovskites originates from a combination of intrinsic material properties and extrinsic experimental factors [21, 23, 38]. From the materials perspective, microstructure plays a main role: grain boundaries in polycrystalline films can act as preferential ion migration pathways, often yielding lower apparent activation energies compared to single crystals or highly oriented large-grain films [23, 60]. In addition, compositional engineering, including halide mixing, A-site cation substitution, and reduced dimensionality (e.g., 2D/3D heterostructures), affects defect formation energies and migration barriers, further broadening the reported range [23, 60]. From the experimental perspective, electrode geometry and interfacial phenomena introduce substantial differences. Asymmetric contacts and interfacial ion accumulation can lead to non-uniform electric fields and strongly influence the observed electrical response [61]. Moreover, measurement artifacts remain a major source of variability: incomplete separation of ionic and electronic contributions, frequency-, or time-scale-dependent probing, and differing data analysis approaches can all yield inconsistent values [62]. Together, these factors underscore the need for standardized measurement protocols and careful reporting of microstructural and device parameters to enable meaningful comparison across studies.

In summary, ion migration in LHPs is governed by a complex interplay of intrinsic material characteristics and extrinsic experimental factors, leading to significant variability in reported activation energies. Establishing consistent methodologies and structure–property relationships will be essential for reliably assessing and controlling ionic transport in these systems.

3 | Methods for Assessing LHP Mixed Conductors

The mixed conduction of LHPs and halide perovskites can, in general, be analyzed using a combination of direct current (DC) galvanostatic polarization and alternating current (AC) impedance spectroscopy. The former technique requires applying a constant square-wave current during the measurement while recording the corresponding voltage response over time. If the studied sample behaves as a purely electronic conductor, the resulting voltage profile exhibits a square-wave form (Figure 4a), with the maximum voltage determined by Ohm's law. Electrical conductivity can then be calculated using Equation (1), where A represents the electrode overlap area and l the spacing between the electrode fingers. To ensure the validity of Ohm's law and maintain linearity, polarization measurements should be performed at low voltages, a condition particularly important for semiconducting materials. For mixed conductors, however, the voltage response deviates from the ideal square-wave pattern (Figure 4b). The transient voltage behavior in this case arises from chemical diffusion processes, which can be modeled using a simplified equivalent circuit (Figure 4c).

$$\sigma = \frac{I}{U}\frac{l}{A} \tag{1}$$

According to this model, the polarization process can be divided into three distinct stages. Initially, upon application of the current, charge transport occurs through both the electronic (R_{eon}) and ionic (R_{ion}) resistance pathways, producing an instantaneous voltage jump (V_{jump}) corresponding to the total resistance R_{tot} (Equation 2).

$$R_{tot} = \frac{R_{eon}\,R_{ion}}{R_{eon} + R_{ion}} \tag{2}$$

Subsequently, the system exhibits an exponential voltage with a characteristic time constant associated with ionic relaxation processes (τ^δ) defined by Equation (3).

$$\tau^\delta = R^\delta C^\delta \tag{3}$$

In the case of stoichiometric polarization, the chemical resistance (presenting the resistance associated with ionic transport and chemical diffusion processes) R^δ (Equation 4) is multiplied with the chemical capacitance (C^δ) (Figure 4c and Equation 3). Once the polarization process is complete, the voltage attains a saturation value (V_{sat}), indicating that the current is conducted exclusively through the electronic resistance (R_{eon}). From these parameters, the ionic conductivity (σ_{ion}) can be determined (using Equation 5).

$$R^\delta = R_{eon} + R_{ion} \tag{4}$$

$$\sigma_{ion} = \sigma_{tot} - \sigma_{eon} \tag{5}$$

Alternatively, AC impedance spectroscopy offers complementary insights to those obtained from DC polarization measurements,

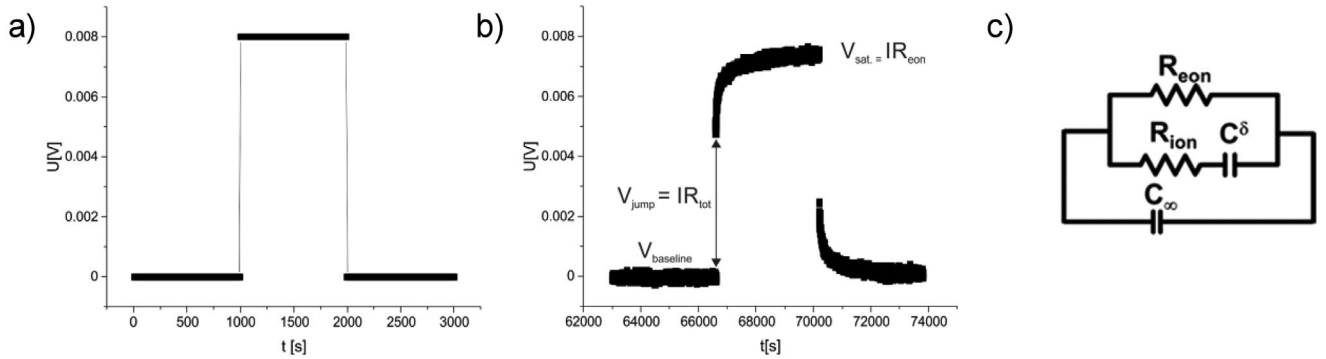

FIGURE 4 | Galvanostatic polarization response. (a) Ideal voltage response of a purely electronic conductor under a constant applied current. (b) Typical voltage response of a mixed ionic–electronic conductor, showing the voltage jump associated with the total resistance and the subsequent evolution toward a steady state. (c) Simplified equivalent circuit models describing charge transport in a mixed conductor, including the electronic resistance (R_{eon}), ionic resistance (R_{ion}), chemical capacitance (C^{δ}), and the high-frequency geometric capacitance of the device, associated with the dielectric response of the bulk material (C_{∞}) (adopted from the references [35, 55, 63]).

with enhanced resolution at high frequency (fast time scale) region. It involves applying a small-amplitude oscillating voltage to the device and recording the resulting frequency-dependent current response. The complex impedance is calculated as the ratio of the voltage amplitude to the complex current, incorporating both magnitude and phase information. In prior studies on halide perovskite films using planar (horizontal) device configurations, space-charge polarization was identified as the rate-limiting mechanism. The response of mixed ionic–electronic conductors is typically represented in the complex plane (Nyquist plot), where distinct features correspond to different transport processes [64]. At high frequencies, the response is dominated by bulk properties, reflecting the total conductivity (ionic and electronic contributions) and geometric capacitance. At lower frequencies, ionic carriers accumulate at the electrode interfaces, leading to polarization effects that appear as an additional semicircle or tail in the spectrum [65, 66]. Under these conditions, the low-frequency response is largely governed by electronic conduction due to ion-blocking contacts. By fitting the impedance spectra with appropriate equivalent circuit models, individual resistive and capacitive contributions associated with ionic and electronic processes can be extracted. While DC polarization enables direct separation of ionic and electronic conductivities in the time domain via transient analysis, AC impedance spectroscopy resolves these contributions in the frequency domain, allowing identification of individual transport processes and access to faster dynamics not captured by DC measurements. The combination of the two techniques, therefore, provides a comprehensive characterization of mixed-conduction behavior in LHPs. For consistency with the DC analysis, the impedance data were analyzed using the equivalent circuit model (Figure 4c). The activation energies for ionic and electronic conduction can be extracted using the Nernst–Einstein relation (Equation 6).

$$\sigma\ (T) = \frac{\sigma_0}{T} exp\left(\frac{-E_A}{kT}\right) \tag{6}$$

where σ_0 is a prefactor, k is the Boltzmann constant, E_A is the activation energy, and T is the temperature. LHPs exhibit higher activation energies for iodide defects (up to ~0.84 eV) [24, 44] compared to 3D counterparts ($MAPbI_3$ shows much lower and widely scattered activation energies (0.2–0.6 eV) [39, 52, 56]). This confirms that dimensionality reduction effectively suppresses ion migration, though the extent of suppression varies with distortion, grain boundaries, and orientation. Overall, the broad ranges and differing trends arise from variations in structure, morphology, and measurement methods. Nonetheless, the combination of DC polarization and AC impedance spectroscopy provides a comprehensive framework for investigating ionic and electronic contributions in LHPs. These methodologies are essential for quantitatively linking defect chemistry and structural properties to mixed conduction behavior.

4 | Application of LHPs as Mixed Conductors

The capacity of LHPs to reduce ion migration in perovskite solar cells stimulated increasing interest in applying mixed-dimensional perovskite architectures to stabilize high-performing perovskite devices [67, 68]. Although ion migration is often viewed as detrimental in devices such as solar cells, the mixed ionic–electronic conductivity of hybrid perovskites also offers opportunities for emerging applications, including resistive-switching devices and energy-storage systems [4, 69]. In resistive switches, ion migration enables reversible transitions between high-resistance and low-resistance states (HRS and LRS, respectively) [70, 71]. These devices can function as so-called memristors, which integrate information storage and processing within a single unit, achieving low-power operation and high computational efficiency analogous to biological synapses. Such brain-inspired behavior underpins the development of next-generation non-volatile neuromorphic computing architectures [3]. In a recent study, Ganaie et al. showed that layered benzylammonium-based perovskites can serve as active resistive-switching media, exhibiting stable digital or analog switching depending on the halide composition [72]. Their devices operated at low voltages with good retention and reproducible cycling, including reliable synaptic operation in lead-free layered hybrid perovskite neuromorphic systems [73, 74]. In particular, halide perovskite devices switch between HRS and LRS states through conductive filament formation/disruption (Figure 5a) and exhibit stable bipolar switching (Figure 5b) and retention behavior (Figure 5c). Furthermore, Loizos et al. demonstrated

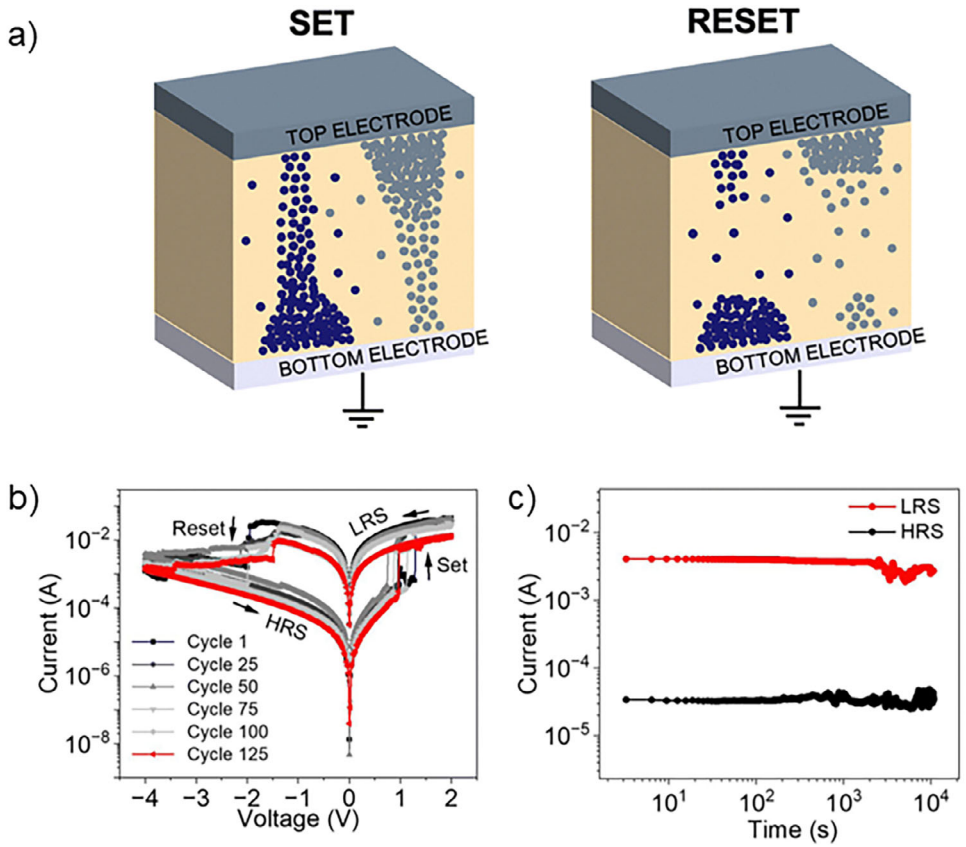

FIGURE 5 | LHPs as mixed conductors in neuromorphic systems. (a) Illustration of the resistive switching process. The diagram shows how halide perovskite memory devices switch between states through the creation (SET) and disruption (RESET) of conductive filaments in the active perovskite layer. These filaments arise from ion vacancies (blue) and metal cations (grey). The perovskite active layer is depicted in light orange. Adopted from Refs. [72, 73] Copyright 2024 Royal Society of Chemistry. (b) Current–voltage characteristics of the bromide-based 2D devices showing bipolar digital switching (between high resistance, HRS, and low resistance, LRS, states), and (c) their retention time over repeated cycles for resistive switching devices at 0.2 V bias showing stable device state operation. Adopted from Refs. [72, 73]. Copyright 2024 Royal Society of Chemistry.

that coating 3D perovskite films with a thin 2D capping layer based on perfluoroarene organic cations significantly improves the durability of resistive-switching devices [75]. They formed mixed-dimensional heterostructures (with mixed 2D and 3D perovskites) that could be used in novel memristor devices that could simultaneously operate as solar cells toward self-powered memories. The treated devices showed much better endurance (up to 10^4 switching cycles vs. ~10^3 for control) and longer state retention. This demonstrates that LHPs can support memory behavior and emulate basic synaptic functions for neuromorphic applications. However, several challenges remain for practical implementation [21, 76]. For example, filament instability, driven by uncontrolled ion migration, can lead to erratic switching behavior and device failure over time. In addition, the kinetics of halide redistribution during repeated cycling can cause gradual degradation of the resistive states, limiting long-term reliability. Moreover, cycling endurance—the ability to maintain stable HRS/LRS states over many cycles—is often compromised by cumulative structural and compositional changes in the perovskite layer, particularly under thermal or electrical stress. These issues persist in mixed-dimensional architectures, where interfacial mismatch or strain between 2D and 3D layers can introduce additional defect sites, accelerating ion migration and filament dissolution, and require further investigation and material engineering to overcome in the future.

To this end, mixed ionic–electronic conduction of halide perovskites enables unique functionalities, although it remains a significant challenge for device stability. Ion migration under light, bias, or heat stress induces hysteresis and device degradation, yet its mechanisms and extent remain poorly understood [3, 4]. Future research should focus on clarifying ionic-electron interactions through advanced in-situ measurement techniques of materials and devices, while introducing standardized protocols. Strategies such as compositional and interface engineering, low-dimensional heterostructures, and strain modulation can further mitigate ion migration [24, 33, 77]. At the same time, controlled ionic motion presents opportunities for new applications, such as resistive switches and memristors, and photo-batteries, among others [3, 78–80]. Balancing control of detrimental ionic effects with the exploitation of beneficial mixed conduction is key to advancing perovskite materials and devices, stimulating further investigations in the research community.

In conclusion, LHPs present a dual character in which reduced ion migration improves device stability, while controlled ionic motion facilitates emerging functionalities such as memristive behavior. Effectively balancing these competing effects will be critical for advancing both stable optoelectronic devices and novel mixed-conductor applications.

5 | Conclusions

Dimensional reduction has already proven highly effective in suppressing ionic mobility in LHPs, leading to markedly improved operational stability compared to their 3D counterparts. However, balancing this reduced ion migration with efficient charge transport remains a challenge. Further progress will depend on optimizing charge transfer, defect passivation, and dielectric confinement to preserve electronic performance while maintaining operational stability. Continued advances in designing organic moieties that are responsive to external stimuli and methodologies to monitor their mixed conduction in functional devices will guide the development of robust perovskite technologies for next-generation photovoltaic and mixed-conductor applications. This opens new avenues for better understanding, controlling, and exploiting the mixed conductivities of layered halide perovskites in the future.

Author Contributions

All authors contributed to developing and writing this perspective article.

Acknowledgments

The authors appreciate the invitation of the Editorial Team to contribute an article to the special issue of the journal. J.V.M. acknowledges the European Research Commission Starting Grant under the Horizon Europe innovation program (no. 101114653, SmartHyMat).

Open access publishing facilitated by Turun yliopisto, as part of the Wiley - FinELib agreement.

Conflicts of Interest

The authors declare no conflicts of interest.

Data Availability Statement

The data that support the findings of this study are available from the corresponding author upon reasonable request.

References

1. M. Grätzel, "The Rise of Highly Efficient and Stable Perovskite Solar Cells," *Accounts of Chemical Research* 50 (2017): 487–491, https://doi.org/10.1021/acs.accounts.6b00492.

2. A. K. Jena, A. Kulkarni, and T. Miyasaka, "Halide Perovskite Photovoltaics: Background, Status, and Future Prospects," *Chemical Reviews* 119 (2019): 3036–3103, https://doi.org/10.1021/acs.chemrev.8b00539.

3. M. H. Futscher and J. V. Milić, "Mixed Conductivity of Hybrid Halide Perovskites: Emerging Opportunities and Challenges," *Frontiers in Energy Research* 9 (2021): 629074, https://doi.org/10.3389/fenrg.2021.629074.

4. W. Tress, "Metal Halide Perovskites as Mixed Electronic–Ionic Conductors: Challenges and Opportunities—From Hysteresis to Memristivity," *Journal of Physical Chemistry Letters* 8 (2017): 3106–3114, https://doi.org/10.1021/acs.jpclett.7b00975.

5. C. Zhang and N.-G. Park, "Materials and Methods for Cost-Effective Fabrication of Perovskite Photovoltaic Devices," *Communications Materials* 5 (2024): 194, https://doi.org/10.1038/s43246-024-00636-8.

6. J.-P. Correa-Baena, M. Saliba, T. Buonassisi, et al., "Promises and Challenges of Perovskite Solar Cells," *Science* 358 (2017): 739–744, https://doi.org/10.1126/science.aam6323.

7. N.-G. Park, M. Grätzel, T. Miyasaka, K. Zhu, and K. Emery, "Towards Stable and Commercially Available Perovskite Solar Cells," *Nature Energy* 1 (2016): 16152, https://doi.org/10.1038/nenergy.2016.152.

8. T. Li, F. He, J. Liang, and Y. Qi, "Functional Layers in Efficient and Stable Inverted Tin-Based Perovskite Solar Cells," *Joule* 7 (2023): 1966–1991, https://doi.org/10.1016/j.joule.2023.08.002.

9. H. Chen, C. Liu, J. Xu, et al., "Improved Charge Extraction in Inverted Perovskite Solar Cells With Dual-Site-Binding Ligands," *Science* 384 (2024): 189–193, https://doi.org/10.1126/science.adm9474.

10. A. Kojima, K. Teshima, Y. Shirai, and T. Miyasaka, "Organometal Halide Perovskites as Visible-Light Sensitizers for Photovoltaic Cells," *Journal of the American Chemical Society* 131 (2009): 6050–6051, https://doi.org/10.1021/ja809598r.

11. M. Grätzel, "The Light and Shade of Perovskite Solar Cells," *Nature Materials* 13 (2014): 838–842, https://doi.org/10.1038/nmat4065.

12. M. Saliba, T. Matsui, J.-Y. Seo, et al., "Cesium-containing Triple Cation Perovskite Solar Cells: Improved Stability, Reproducibility and High Efficiency," *Energy & Environmental Science* 9 (2016): 1989–1997, https://doi.org/10.1039/C5EE03874J.

13. J. Wei, Q. Wang, J. Huo, et al., "Mechanisms and Suppression of Photoinduced Degradation in Perovskite Solar Cells," *Advanced Energy Materials* 11 (2021): 2002326, https://doi.org/10.1002/aenm.202002326.

14. Y. Rong, Y. Hu, A. Mei, et al., "Challenges for Commercializing Perovskite Solar Cells," *Science* 361 (2018): eaat8235, https://doi.org/10.1126/science.aat8235.

15. K. Domanski, B. Roose, T. Matsui, et al., "Migration of Cations Induces Reversible Performance Losses Over Day/Night Cycling in Perovskite Solar Cells," *Energy & Environmental Science* 10 (2017): 604–613, https://doi.org/10.1039/C6EE03352K.

16. K. Domanski, J.-P. Correa-Baena, N. Mine, et al., "Not All That Glitters Is Gold: Metal-Migration-Induced Degradation in Perovskite Solar Cells," *ACS Nano* 10 (2016): 6306–6314, https://doi.org/10.1021/acsnano.6b02613.

17. D. Moia and J. Maier, "Ion Transport, Defect Chemistry, and the Device Physics of Hybrid Perovskite Solar Cells," *ACS Energy Letters* 6 (2021): 1566–1576, https://doi.org/10.1021/acsenergylett.1c00227.

18. S. Tammireddy, M. N. Lintangpradipto, O. Telschow, et al., "Hysteresis and Its Correlation to Ionic Defects in Perovskite Solar Cells," *The Journal of Physical Chemistry Letters* 15 (2024): 1363–1372, https://doi.org/10.1021/acs.jpclett.3c03146.

19. A. Pockett and M. J. Carnie, "Ionic Influences on Recombination in Perovskite Solar Cells," *ACS Energy Letters* 2 (2017): 1683–1689, https://doi.org/10.1021/acsenergylett.7b00490.

20. J. Thiesbrummel, S. Shah, E. Gutierrez-Partida, et al., "Ion-induced Field Screening as a Dominant Factor in Perovskite Solar Cell Operational Stability," *Nature Energy* 9 (2024): 664–676, https://doi.org/10.1038/s41560-024-01487-w.

21. F. Li, Y. Liang, and R. Zheng, "A Balanced View of Ion Migration in Halide Perovskite Electronics," *Newton* 1 (2025): 100096.

22. D. W. Ferdani, S. R. Pering, D. Ghosh, et al., "Partial Cation Substitution Reduces Iodide Ion Transport in Lead Iodide Perovskite Solar Cells," *Energy & Environmental Science* 12 (2019): 2264–2272, https://doi.org/10.1039/C9EE00476A.

23. Y. Lin, Y. Bai, Y. Fang, Q. Wang, Y. Deng, and J. Huang, "Suppressed Ion Migration in Low-Dimensional Perovskites," *ACS Energy Letters* 2 (2017): 1571–1572, https://doi.org/10.1021/acsenergylett.7b00442.

24. A. Dučinskas, M. Jung, Y.-R. Wang, et al., "Mixed Ionic-electronic Conduction in Ruddlesden–Popper and Dion–Jacobson Layered Hybrid Perovskites With Aromatic Organic Spacers," *Journal of Materials Chemistry C* 12 (2024): 7909–7915, https://doi.org/10.1039/D4TC01010H.

25. G. AlSabeh, V. Slama, M. Ren, et al., "Aryl-Acetylene Layered Hybrid Perovskites in Photovoltaics," *Angewandte Chemie International Edition* 64 (2025): e202417432, https://doi.org/10.1002/anie.202417432.

26. Y. Yuan and J. Huang, "Ion Migration in Organometal Trihalide Perovskite and Its Impact on Photovoltaic Efficiency and Stability," *Accounts of Chemical Research* 49 (2016): 286–293, https://doi.org/10.1021/acs.accounts.5b00420.

27. G. AlSabeh, V. Slama, M. Almalki, et al., "On the Accessibility of Higher- n Phases in Formamidinium-Based Ruddlesden-Popper and Dion–Jacobson Layered Hybrid Perovskites," *Advanced Electronic Materials* 11 (2025): e00164, https://doi.org/10.1002/aelm.202500164.

28. G. Grancini and M. K. Nazeeruddin, "Dimensional Tailoring of Hybrid Perovskites for Photovoltaics," *Nature Reviews Materials* 4 (2019): 4–22, https://doi.org/10.1038/s41578-018-0065-0.

29. B. Saparov and D. B. Mitzi, "Organic–Inorganic Perovskites: Structural Versatility for Functional Materials Design," *Chemical Reviews* 116 (2016): 4558–4596, https://doi.org/10.1021/acs.chemrev.5b00715.

30. C. C. Stoumpos, D. H. Cao, D. J. Clark, et al., "Ruddlesden–Popper Hybrid Lead Iodide Perovskite 2D Homologous Semiconductors," *Chemistry of Materials* 28 (2016): 2852–2867, https://doi.org/10.1021/acs.chemmater.6b00847.

31. L. Mao, W. Ke, L. Pedesseau, et al., "Hybrid Dion–Jacobson 2D Lead Iodide Perovskites," *Journal of the American Chemical Society* 140 (2018): 3775–3783, https://doi.org/10.1021/jacs.8b00542.

32. J. V. Milić, S. M. Zakeeruddin, and M. Grätzel, "Layered Hybrid Formamidinium Lead Iodide Perovskites: Challenges and Opportunities," *Accounts of Chemical Research* 54 (2021): 2729–2740.

33. W. Luo, G. AlSabeh, and J. V. Milić, "Supramolecular Control in Hybrid Perovskite Photovoltaics," *Photochemistry* 50 (2022): 342–366.

34. H. J. Snaith, "Present Status and Future Prospects of Perovskite Photovoltaics," *Nature Materials* 17 (2018): 372–376, https://doi.org/10.1038/s41563-018-0071-z.

35. A. Senocrate and J. Maier, "Solid-State Ionics of Hybrid Halide Perovskites," *Journal of the American Chemical Society* 141 (2019): 8382–8396, https://doi.org/10.1021/jacs.8b13594.

36. J. Thiesbrummel, J. V. Milić, C. Deibel, et al., "Ion Migration in Perovskite Solar Cells," *Nature Reviews Chemistry* 10 (2026): 179–195, https://doi.org/10.1038/s41570-025-00790-8.

37. J. L. Minns, P. Zajdel, D. Chernyshov, W. Van Beek, and M. A. Green, "Structure and Interstitial Iodide Migration in Hybrid Perovskite Methylammonium Lead Iodide," *Nature Communications* 8 (2017): 15152, https://doi.org/10.1038/ncomms15152.

38. A. Walsh, D. O. Scanlon, S. Chen, X. G. Gong, and S.-H. Wei, "Self-Regulation Mechanism for Charged Point Defects in Hybrid Halide Perovskites," *Angewandte Chemie International Edition* 54 (2015): 1791–1794, https://doi.org/10.1002/anie.201409740.

39. M. H. Futscher, J. M. Lee, L. McGovern, et al., "Quantification of Ion Migration in $CH_3NH_3PbI_3$ Perovskite Solar Cells by Transient Capacitance Measurements," *Materials Horizons* 6 (2019): 1497–1503, https://doi.org/10.1039/C9MH00445A.

40. J. M. Azpiroz, E. Mosconi, J. Bisquert, and F. De Angelis, "Defect Migration in Methylammonium Lead Iodide and Its Role in Perovskite Solar Cell Operation," *Energy & Environmental Science* 8 (2015): 2118–2127, https://doi.org/10.1039/C5EE01265A.

41. J. Y. Park, Y. H. Lee, M. A. Z. Mamun, et al., "Electrically Induced Directional Ion Migration in Two-Dimensional Perovskite Heterostructures," *Matter* 7 (2024): 1817–1832.

42. T. L. Leung, I. Ahmad, A. A. Syed, A. M. C. Ng, J. Popović, and A. B. Djurišić, "Stability of 2D and Quasi-2D Perovskite Materials and Devices," *Communications Materials* 3 (2022): 63, https://doi.org/10.1038/s43246-022-00285-9.

43. X. Xiao, J. Dai, Y. Fang, et al., "Suppressed Ion Migration Along the in-Plane Direction in Layered Perovskites," *ACS Energy Letters* 3 (2018): 684–688, https://doi.org/10.1021/acsenergylett.8b00047.

44. J. Cho, J. T. DuBose, A. N. T. Le, and P. V. Kamat, "Suppressed Halide Ion Migration in 2D Lead Halide Perovskites," *ACS Materials Letters* 2 (2020): 565–570, https://doi.org/10.1021/acsmaterialslett.0c00124.

45. D. Zhang, D. Li, Y. Hu, A. Mei, and H. Han, "Degradation Pathways in Perovskite Solar Cells and How to Meet International Standards," *Communications Materials* 3 (2022): 58, https://doi.org/10.1038/s43246-022-00281-z.

46. A. Mishra, A. Paramvir, G. C. Fish, et al., "Naphthalenediimide/Formamidinium-Based Low-Dimensional Perovskites," *Chemistry of Materials* 33 (2021): 6412–6420, https://doi.org/10.1021/acs.chemmater.1c01635.

47. Y. Wang, A. Senocrate, M. Mladenović, et al., "Photo De-Mixing in Dion-Jacobson 2D Mixed Halide Perovskites," *Advanced Energy Materials* 12 (2022): 2200768.

48. Z. Chen, G. Brocks, S. Tao, and P. A. Bobbert, "Unified Theory for Light-Induced Halide Segregation in Mixed Halide Perovskites," *Nature Communications* 12 (2021): 2687, https://doi.org/10.1038/s41467-021-23008-z.

49. E. M. Hutter, L. A. Muscarella, F. Wittmann, et al., "Thermodynamic Stabilization of Mixed-Halide Perovskites Against Phase Segregation," *Cell Reports Physical Science* 1 (2020): 100120, https://doi.org/10.1016/j.xcrp.2020.100120.

50. E. T. Hoke, D. J. Slotcavage, E. R. Dohner, A. R. Bowring, H. I. Karunadasa, and M. D. McGehee, "Reversible Photo-Induced Trap Formation in Mixed-Halide Hybrid Perovskites for Photovoltaics," *Chemical Science* 6 (2015): 613–617, https://doi.org/10.1039/C4SC03141E.

51. J. Cho, M. Mukherjee, G. Szabó, S. Min, and P. V. Kamat, "Stabilizing Iodine in 2D Mixed Halide Perovskites: Dion–Jacobson versus Ruddlesden–Popper Phases," *Advanced Optical Materials* 14 (2026): e03619, https://doi.org/10.1002/adom.202503619.

52. A. Senocrate, I. Moudrakovski, G. Y. Kim, et al., "The Nature of Ion Conduction in Methylammonium Lead Iodide: A Multimethod Approach," *Angewandte Chemie* 129 (2017): 7863–7867, https://doi.org/10.1002/ange.201701724.

53. A. Senocrate, T.-Y. Yang, G. Gregori, G. Y. Kim, M. Grätzel, and J. Maier, "Charge Carrier Chemistry in Methylammonium Lead Iodide," *Solid State Ionics* 321 (2018): 69–74, https://doi.org/10.1016/j.ssi.2018.03.029.

54. J.-W. Lee, S. Tan, S. I. Seok, Y. Yang, and N.-G. Park, "Rethinking the A Cation in Halide Perovskites," *Science* 375 (2022): eabj1186, https://doi.org/10.1126/science.abj1186.

55. A. Dučinskas, Structure-property Relationships and Mixed Conductivity in Layered Hybrid Perovskites Based on Phenyl-derived Spacers (2022) EPFL.

56. C. Eames, J. M. Frost, P. R. F. Barnes, B. C. O'Regan, A. Walsh, and M. S. Islam, "Ionic Transport in Hybrid Lead Iodide Perovskite Solar Cells," *Nature Communications* 6 (2015): 7497, https://doi.org/10.1038/ncomms8497.

57. A. Mahapatra, R. Runjhun, J. Nawrocki, et al., "Elucidation of the Role of Guanidinium Incorporation in Single-Crystalline $MAPbI_3$ Perovskite on Ion Migration and Activation Energy," *Physical Chemistry Chemical Physics* 22 (2020): 11467–11473, https://doi.org/10.1039/D0CP01119C.

58. A. Dučinskas, G. Y. Kim, D. Moia, et al., "Unravelling the Behavior of Dion–Jacobson Layered Hybrid Perovskites in Humid Environments," *ACS Energy Letters* 6 (2020): 337–344, https://doi.org/10.1021/acsenergylett.0c02344.

59. S. Ahmad, P. Fu, S. Yu, et al., "Dion-Jacobson Phase 2D Layered Perovskites for Solar Cells With Ultrahigh Stability," *Joule* 3 (2019): 794–806, https://doi.org/10.1016/j.joule.2018.11.026.

60. E. Mosconi and F. De Angelis, "Mobile Ions in Organohalide Perovskites: Interplay of Electronic Structure and Dynamics," *ACS Energy Letters* 1 (2016): 182–188, https://doi.org/10.1021/acsenergylett.6b00108.

61. P. Calado, A. M. Telford, D. Bryant, et al., "Evidence for Ion Migration in Hybrid Perovskite Solar Cells With Minimal Hysteresis," *Nature Communications* 7 (2016): 13831, https://doi.org/10.1038/ncomms13831.

62. N. Yantara and N. Mathews, "Toolsets for Assessing Ionic Migration in Halide Perovskites," *Joule* 8 (2024): 1239–1273, https://doi.org/10.1016/j.joule.2024.02.022.

63. D. Moia, M. Jung, Y.-R. Wang, and J. Maier, "Ionic and Electronic Polarization Effects in Horizontal Hybrid Perovskite Device Structures Close to Equilibrium," *Physical Chemistry Chemical Physics* 25 (2023): 13335–13350, https://doi.org/10.1039/D3CP01182H.

64. J. Maier, *Physical Chemistry of Ionic Materials: Ions and Electrons in Solids* (John Wiley & Sons, 2023).

65. A. Bou, A. Pockett, D. Raptis, T. Watson, M. J. Carnie, and J. Bisquert, "Beyond Impedance Spectroscopy of Perovskite Solar Cells: Insights From the Spectral Correlation of the Electrooptical Frequency Techniques," *Journal of Physical Chemistry Letters* 11 (2020): 8654–8659, https://doi.org/10.1021/acs.jpclett.0c02459.

66. P. Lopez-Varo, J. A. Jiménez-Tejada, M. García-Rosell, et al., "Device Physics of Hybrid Perovskite Solar Cells: Theory and Experiment," *Advanced Energy Materials* 8 (2018): 1702772, https://doi.org/10.1002/aenm.201702772.

67. S. Teale, M. Degani, B. Chen, E. H. Sargent, and G. Grancini, "Molecular Cation and Low-Dimensional Perovskite Surface Passivation in Perovskite Solar Cells," *Nature Energy* 9 (2024): 779–792, https://doi.org/10.1038/s41560-024-01529-3.

68. G. Grancini, C. Roldán-Carmona, I. Zimmermann, et al., "One-Year Stable Perovskite Solar Cells by 2D/3D Interface Engineering," *Nature Communications* 8 (2017): 15684, https://doi.org/10.1038/ncomms15684.

69. X. Zhao, H. Xu, Z. Wang, Y. Lin, and Y. Liu, "Memristors With Organic-Inorganic Halide Perovskites," *InfoMat* 1 (2019): 183–210, https://doi.org/10.1002/inf2.12012.

70. X. Zhu, J. Lee, and W. D. Lu, "Iodine Vacancy Redistribution in Organic–Inorganic Halide Perovskite Films and Resistive Switching Effects," *Advanced Materials* 29 (2017): 1700527, https://doi.org/10.1002/adma.201700527.

71. F. Ma, Y. Zhu, Z. Xu, et al., "Optoelectronic Perovskite Synapses for Neuromorphic Computing," *Advanced Functional Materials* 30 (2020): 1908901, https://doi.org/10.1002/adfm.201908901.

72. M. M. Ganaie, G. Bravetti, S. Sahu, M. Kumar, and J. V. Milić, "Resistive Switching in Benzylammonium-Based Ruddlesden–Popper Layered Hybrid Perovskites for Non-Volatile Memory and Neuromorphic Computing," *Materials Advances* 5 (2024): 1880–1886, https://doi.org/10.1039/D3MA00618B.

73. M. Loizos, K. Rogdakis, W. Luo, et al., "Resistive Switching Memories With Enhanced Durability Enabled by Mixed-Dimensional Perfluoroarene Perovskite Heterostructures," *Nanoscale Horizons* 9 (2024): 1146–1154, https://doi.org/10.1039/D4NH00104D.

74. M. Ghasemi, G. Bravetti, M. Loizos, et al., "Mechanosynthesis of Layered Double Perovskites With Aromatic Spacer Cations for Lead-Free Thin-Film Opto(electro)Ionics," *ChemPhysChem* 27 (2026): e202500764, https://doi.org/10.1002/cphc.202500764.

75. M. M. Ganaie, M. Mohammadi, M. Loizos, et al., "Lead-Free Layered Halide Double Perovskites With Aromatic Organic Cations for Resistive Switching Memories and Artificial Synapses," *Materials Horizons* 13 (2026): 5010–5021, https://doi.org/10.1039/D5MH02220G.

76. N. Yantara, X. Xing, D. Sharma, D. J. J. Tay, S. Varku, and N. Mathews, "From Solar Cells to Memristors: Halide Perovskites as a Platform for Neuromorphic Electronics," *Chemical Society Reviews* 55 (2026): 2145–2228, https://doi.org/10.1039/D5CS01222H.

77. H. Zhang, M. K. Nazeeruddin, and W. C. Choy, "Perovskite Photovoltaics: The Significant Role of Ligands in Film Formation, Passivation, and Stability," *Advanced Materials* 31 (2019): 1805702, https://doi.org/10.1002/adma.201805702.

78. X. Zhao, Z. Wang, W. Li, et al., "Photoassisted Electroforming Method for Reliable Low-Power Organic–Inorganic Perovskite Memristors"," *Advanced Functional Materials* 30 (2020): 1910151.

79. Z. Xiao and J. Huang, "Energy-Efficient Hybrid Perovskite Memristors and Synaptic Devices," *Advanced Electronic Materials* 2 (2016): 1600100, https://doi.org/10.1002/aelm.201600100.

80. S. Ahmad, C. George, D. J. Beesley, J. J. Baumberg, and M. De Volder, "Photo-Rechargeable Organo-Halide Perovskite Batteries," *Nano Letters* 18 (2018): 1856–1862, https://doi.org/10.1021/acs.nanolett.7b05153.

Biographies

Dr. Ghewa AlSabeh is a postdoctoral researcher at the Laboratory of Photonics and Interfaces at École Polytechnique Fédérale de Lausanne (EPFL) since September, 2025. She obtained her MSc degree at the American University of Beirut in Lebanon in 2020 and her doctoral degree at EPFL in 2025, working as a doctoral researcher at the Laboratory of Photonics and Interfaces and the Smart Energy Materials group at the Adolphe Merkle Institute of the University of Fribourg in Switzerland under the supervision of Prof. Jovana V. Milić and Prof. Michael Graetzel. Her research has been focused on the multifunctionality of layered perovskites and their light-induced transformations in emerging technologies.

Dr. Algirdas Dučinskas obtained his PhD in Physical Chemistry from EPFL in 2022 under the supervision of Prof. Michael Graetzel and the co-supervision of Dr. Jovana V. Milić. He has conducted research at the Max Planck Institute for Solid State Research and the group of Prof. Joachim Maier. His research focused on structure–property relationships and mixed conductivity in layered hybrid perovskites. His work advances the understanding of optoelectronic materials for applications in photovoltaics and memristive devices.

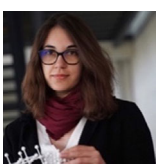

Prof. Jovana V. Milić has been an Associate Professor at the Department of Chemistry of the University of Turku in Finland since September, 2024. She obtained her PhD in Chemistry at ETH Zurich in 2017 and, since then, she has worked as a scientist in the Laboratory of Photonics and Interfaces at EPFL until 2020, when she became Assistant Professor (SNSF PRIMA Fellow) at the Adolphe Merkle Institute of the University of Fribourg in Switzerland. Her research is centered on developing stimuli–responsive supramolecular materials for energy conversion, with a particular focus on halide perovskites and their use in energy and smart (nano)technologies.

Prof. Michael Graetzel is director of the Laboratory of Photonics and Interfaces at EPFL. He is a pioneer of molecular photovoltaics, having conceived and realized mesoscopic photosystems that use molecular light harvesters to convert sunlight into electricity. His introduction of the dye-sensitized solar cell (DSSC or "Graetzel cell") shifted photovoltaics beyond traditional p–n junctions to a molecular-level approach that separates light absorption from charge transport, mimicking natural photosynthesis. These developments played a central role in the emergence of perovskite solar cells. Beyond photovoltaics, he extended mesoscopic concepts to energy storage and solar fuel generation, while ranking among the most influential scientists globally.